Special issue article

Journal of Applied Toxicology

Received: 15 January 2017, Revised: 3 March 2017, Accepted: 17 March 2017 Published online in Wiley Online Library: 9 May 2017

(wileyonlinelibrary.com) DOI 10.1002/jat.3477

Graphene and carbon nanotubes activate different cell surface receptors on macrophages before and after deactivation of endotoxins

Mohamed H. Lahiani[a,b†], Kuppan Gokulan[a*†], Katherine Williams[a], Mariya V. Khodakovskaya[b,c] and Sangeeta Khare[a*]

ABSTRACT: Nanomaterial synthesis and handling in a non-sterile environment can result in the final product becoming contaminated with bacterial endotoxin or lipopolysaccharides (LPB). During toxicological testing, the effects caused by endotoxin-contaminated nanomaterials can be misinterpreted in the end-point analysis (such as cytotoxicity and immune responses) and could result in erroneous conclusions. The objective of this study was twofold: (i) to test different carbon-based nanomaterials (CBNs) [pristine graphene and multi-wall carbon nanotubes (MWCNTs)] for the presence of endotoxin and develop strategies for depyrogenation, and (ii) to compare the immune response exhibited by macrophages after exposure to native CBNs versus depyrogenated CBNs. The gel-clot limulus amebocyte lysate (LAL) and chromogenic-based LAL assays were used to detect endotoxins. Results revealed that the CBNs contained greater amounts of endotoxin than are approved by major regulatory agencies (0.5 EU ml^{-1}). Three repeated cycles of autoclaving reduced the endotoxin in the test materials. Macrophages were incubated with pyrogenated and depyrogenated pristine graphene and MWCNTs to test differences in phagocytosis, cytotoxicity, and expression of genes involved in macrophage activation. The uptake of depyrogenated CBNs was significantly reduced as compared with pyrogenated CBNs. Exposure of macrophages to depyrogenated CBNs resulted in a distinct pattern of gene expression for TLR signaling, NOD-like receptor signaling, and downstream signal transduction molecules. Furthermore, macrophages exposed to both types of CBNs showed the downregulation of *TLR5* and *NLRC4* inflammasomes. The results of this study reaffirm that assessment of endotoxin and other bacterial contamination is critical when evaluating the cellular toxicity of nanomaterials. Published 2017. This article has been contributed to by US Government employees and their work is in the public domain in the USA.

Keywords: endotoxin; graphene; carbon nanotubes; macrophages; cell surface receptor; LAL assay; cytotoxicity

Introduction

Engineered nanomaterials offer a considerable commercial potential for new products such as optical devices, electronics, superconductors, fuel cells, catalysts, biosensors, health care products, and in medical diagnosis tools (Adibkia *et al*., 2007; Tiwari *et al*., 2011; Alex and Tiwari, 2015). Due to the rapid application and wide development of nanotechnology, there are already more than 1300 nanomaterials (NMs) products available on the market (Zhou *et al*., 2014) and this number is predicted to grow exponentially (Zhou *et al*., 2014). In 2014, it was predicted that more than 15% of commercially available products would incorporate some form of nanotechnology during the manufacturing process (Zhou *et al*., 2014; Vance *et al*., 2015). NMs can be classified based on specific chemical and physical properties that include: carbonaceous, semiconductors, metal oxides, lipids, zero-valent metals, quantum dots, non-polymer, nanofibers, nanowires, and nanosheets. In biomedical applications, NMs have tremendous use in drug delivery, tissue engineering, cancer therapy, and enhancing the therapeutic efficacy of drugs (Dizaj *et al*., 2015). Furthermore, metal-based NMs have been employed as an antimicrobial agent against foodborne pathogens, as well as antibiotic resistant bacteria (Vance *et al*., 2015). Some of these nanoparticles are available on the open market as a health supplement, thus raising concerns about the safety of such products for consumer use (Williams *et al*., 2016, 2015; Bekele *et al*., 2016). Currently, carbon-based nanomaterials (CBNs) are among the most widely investigated and used nanomaterials (NMs). Due to their multifunctional nature, CBNs have found a broad range of applications extending from electronics and aerospace to agriculture and medicine. The production of CBNs exceeded 1000 tons in the year 2011 (Aslani *et al*., 2014). Many industries have embraced various CBNs forms, including graphene, single and multi-walled nanotubes, fullerenes, nano-diamonds and nano horns, due to their excellent mechanical strength, thermal conductivity and optical properties (Green and Hersam, 2011; Cha *et al*., 2013; Amenta and Aschberger, 2015). Moreover, CBNs are now being tested for many biomedical applications, including drug delivery, tissue scaffolding and cellular sensors (Bianco *et al*., 2005; Harrison and Atala, 2007; Canas *et al*.,

*Correspondence to: Kuppan Gokulan and Sangeeta Khare, Division of Microbiology, National Center for Toxicological Research, US-FDA, 3900 NCTR Rd, Jefferson, AR, 72079, USA.
E-mail: kuppan.gokulan@fda.hhs.gov; sangeeta.khare@fda.hhs.gov

†Authors contributed equally to the study.

[a]Division of Microbiology, National Center for Toxicological Research, US Food and Drug Administration, Jefferson, AR, 72079, USA

[b]Department of Biology, University of Arkansas at Little Rock, Little Rock, AR, 72204, USA

[c]Institute of Biology and Soil Sciences, Vladivostok, Russian Federation, 690024

2008; Bae *et al.*, 2011; Madani *et al.*, 2011; Cha *et al.*, 2013; Che Abdullah *et al.*, 2014). As the numbers of products using CBNs have increased, so have concerns about the risks associated with the use of these NMs. For this reason, there is growing demand to correctly assess CBNs risks to protect workers, consumers, and the environment.

One of the major concerns in NMs manufacturing is the sterility of the environment in which the material is being synthesized. Even though a large number of publications have addressed the issue of CBNs toxicity, very few have warned about the potential for contamination with endotoxins (Esch *et al.*, 2010; Cha *et al.*, 2013; Zhang *et al.*, 2013; Amenta and Aschberger, 2015; Jackson *et al.*, 2015). Endotoxins are also known as lipopolysaccharide (LPS), an endogenous pyrogen. LPS contamination is found in many chemicals and laboratory glassware (Vallhov *et al.*, 2006). If proper precautions are not taken during CBNs synthesis or purification, LPS can be adsorbed onto the CBNs. Researchers commonly test procured NMs to determine immunogenicity and toxicity using *in vivo*, *in vitro* or *ex vivo* biological test systems. However, the results obtained from such assay could be misleading if the observed activation is due to the contaminating pyrogen, rather than any inherent property of the NMs itself. Indeed, it has been shown that carbon nanotubes have a high binding capacity to *Escherichia coli* endotoxins (357 EU ml^{-1} sorbent ~35.7 ng mg^{-1}) (Ying, 2006; Schaumberger *et al.*, 2014). Bacterial endotoxin that is derived from Gram-negative bacteria binds with TLR4 receptors on immune cells (macrophages or dendritic cells). This interaction triggers the expression of proinflammatory cytokines (*IL-1β, IFN-γ, IL-6 and TNF-α*) and can result in deregulated inflammation and toxicity.

Human beings are unintentionally exposed to NMs through manufacturing, environmental exposure, and food packaging materials, and intentionally through biomedical applications. This continuous exposure to NMs may pose a risk in terms of toxicity. Several *in vitro* and *in vivo* studies have shown that ENMs caused adverse immunotoxicity effects that resulted in cell death. However, there is little information on how host immune cells interact with NMs to induce innate immunity or impact the inflammatory response to promote defence mechanisms. Immune cells must mount an appropriate reaction against foreign agents such as NMs; as an excessive immune response could cause tissue damage, unwanted inflammatory reactions, and disease progression. For example, mice injected with graphene showed cytotoxicity in a dose-dependent manner, with NMs deposited in lung, liver and spleen and resulting in tissue damage (Wang *et al.*, 2011). However, it is not clear if the observed toxicity was induced by the NMs or due to endotoxin contamination. It is necessary to distinguish the cause of immunotoxicity by evaluating: (i) if it is caused by bacterial endotoxin present in the NM; or (ii) if the NM itself is a cause for the toxicity. Both endotoxin and various NMs could bind to distinct host cell surface receptors and alter cellular and immunological function at the molecular level (Chow *et al.*, 1999; Vives-Pi *et al.*, 2003; Tsai *et al.*, 2012; Qu *et al.*, 2013).

This study aimed to evaluate the level of endotoxin in CBNs before and after a depyrogenation procedure. In addition, we also evaluated the immunotoxicity function of macrophages as assessed by phagocytosis, cytotoxicity and changes in the expression of genes related to immune response. The results of this study will help identify toxicity and dose–response information for CBNs, providing information to help evaluate the safety of products containing such materials.

Materials and methods

Materials

Pristine graphene was supplied by the NanoCore facility at the National Center for Toxicological Research (NCTR) in Jefferson, AR, USA and characterized at NCTR and the University of Arkansas at Little Rock (Little Rock, AR, USA). Graphene nanoplatelets (< 3 layers; lateral dimensions 1–2 um), long MWCNTs [MWCNTs-COOH-long (OD 13–18 nm; length 1–12 um)], and short MWCNTs [MWCNT-COOH-short (OD < 7 nm; length 0.5–2 um)] were purchased from Cheap Tubes (Brattleboro, VT, USA). Helical carbon nanotubes [Helical MWCNTs (OD 100–200 nm; length 1–10 um)] were purchased from US Research Nanomaterials Inc (Houston, TX, USA). Single-walled carbon nano horns (SWCNHs) were provided by Dr Puretzky from Oak Ridge National Laboratory (Puretzky *et al.*, 2008). Activated carbon was purchased from Sigma-Aldrich (St. Louis, MO, USA). All CBNs were suspended in water and sonicated for 15 min. After sonication, bovine serum albumin (BSA) was added to these suspensions to achieve a final concentration of 0.05%. The BSA was added to enhance the ability of the CBNs to maintain a uniform suspension.

Endotoxin detection

Endotoxin testing was performed using the ToxinSensor™ Chromogenic LAL Endotoxin Assay Kit from Genescript (Piscataway, NJ, USA) with modification (Fig. 1). Endotoxin detection was performed at four different concentrations of CBNs suspensions (10, 1, 0.1, and 0.01 μg ml^{-1}). Inhibition/Enhancement controls (IEC) were prepared by spiking 0.1 EU into each CBNs solution as described by the FDA/USP guidelines (US-FDA, 2012). After measuring the amount of endotoxin in each concentration, samples (spiked or not spiked) were centrifuged at 10 000 g for 15 min. The supernatant was then collected and retested for the presence of endotoxins. All absorbance readings were performed at 545 nm using the Cytation™ 3 Cell Imaging Multi-Mode Microplate reader (Biotek, Winooski, VT, USA). Qualitative measurement of endotoxin was done using a Gel clot assay kit (ToxinSensor™ Gel Clot Endotoxin Assay Kit; Genescript, Piscataway, NJ, USA).

Endotoxin deactivation by autoclaving

After 100 mg of CBNs was weighed and transferred into a clean, autoclaved vial, 1 ml of sterilized water was added to each sample and the vial sonicated in a water-bath sonicator for 15 min. The sonicated samples were then autoclaved at 120°C for 20 min and this autoclaving procedure was repeated three times as previously described by Barbosa *et al.* (2015). These autoclaved NMs are referred to as depyrogenated or autoclaved (AU-graphene or AU-MWCNT) samples in this manuscript. Control samples were suspended in water and sonicated as described earlier, however, these samples did not undergo any autoclave treatment. These samples are referred to as pyrogenated or non-autoclaved (NA-graphene or NA-MWCNTs) samples.

Macrophage cell culture

J774 mouse macrophage cells (TIB-67; ATCC, Manassas, VA, USA) were grown in 75-cm culture flasks in Dulbecco's modified

Journal of Applied Toxicology

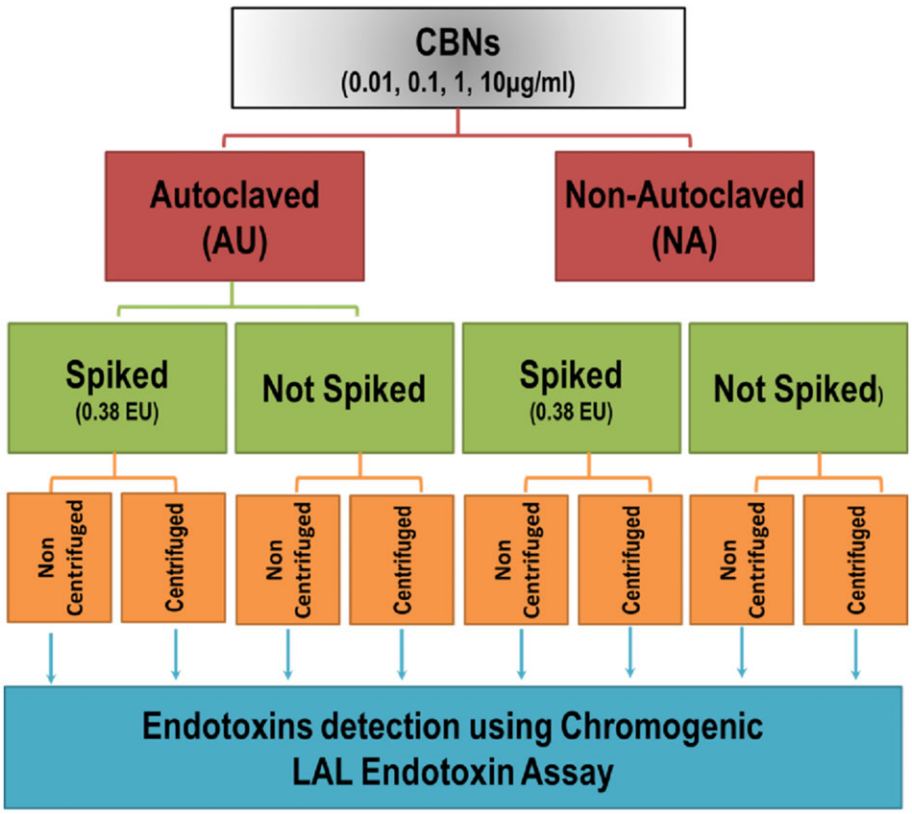

Figure 1. Schematic diagram showing the strategy for endotoxin detection in the test samples. [Colour figure can be viewed at wileyonlinelibrary.com]

Eagle's medium (DMEM) supplemented with 2 mM glutamine, 10% fetal bovine serum (FBS), penicillin (100 units ml^{-1}) and streptomycin (100 µg ml^{-1}). The cells were cultured at 37°C with 5% CO_2 in 95% humidity. After growth, cells were detached from the culture flask using a cell scraper and washed with DMEM. The cell pellet was re-suspended in enriched DMEM and plated into 24-well culture plates (4×10^5 cells per well). The culture plates were incubated at 37°C with 5% CO_2 and 95% humidity for 24 to 48 h.

Treatment of macrophages with CBNs

To test the response of macrophages during CBNs treatment, two different CBNs materials were chosen: pristine graphene and long MWCNTs. Both materials were incubated with J774 mouse macrophages at 1 and 20 µg ml^{-1} concentrations. For comparison, autoclaved MWCNTs (AU-MWCNTs) and autoclaved graphene (AU-graphene) were also incubated with J774 cells for 48 h at 1 and 20 µg ml^{-1} concentrations. Untreated J774 cells and cells incubated with purified endotoxins (1 and 2 EU ml^{-1}) were used as controls.

Expression of genes involved in immune response

J774 mouse macrophages were grown in 25-cm culture flasks (8×10^6 cells per flask) as described in the previous section and macrophages were incubated with autoclaved or non-autoclaved CBNs at a concentration of 1 or 20 µg ml^{-1}. At time points 1, 3, and 48 h post incubation, culture supernatants were removed and stored at −80°C to measure CBNs-induced cell cytotoxicity (as mentioned in the next section). Macrophages were washed twice with pre-warmed media. The cells were then lysed with ice cold TRI-Reagent (Molecular Research Center, Cincinnati, OH, USA) and thoroughly mixed to obtain cell lysate. The RNA extraction was performed as described earlier (Gokulan *et al.*, 2016). The RNA was treated with DNase (Ambion, Austin, TX, USA) to ensure high-quality purified RNA. The quantity of total extracted RNA was quantified using a ND-1000 spectrophotometer (NanoDrop Technologies, Wilmington, DE, USA) and the RNA stored at −80°C until use. cDNA was generated by adding 2 µg of total RNA to a 100-µl reaction containing 2.5 mM of random hexamer and reagents from the Reverse Transcription Kit (Applied Biosystems, Foster City, CA, USA) according to manufacturer's instructions. Evaluation of gene expression was performed using Antibacterial Response PCR Arrays (SA Biosciences/ Qiagen, Valencia, CA, USA) in an Applied Biosystems 7500 DNA Sequence Detection System. Analysis of the PCR data was performed using the PCR Array Data Analysis Software (SA Biosciences).

Cell cytotoxicity assay

Macrophages were incubated with CBNs as described above. Cytotoxicity assays were performed using a CytoTox 96 Non-Radioactive Cytotoxicity Assay kit (Promega, Madison, WI, USA). The cytotoxicity results were expressed in fold difference of lactate dehydrogenase (LDH) activity using the following formula: fold difference = cytotoxicity induced by CBNs/ cytotoxicity of uninfected control cells. Each data point represents the means and standard deviation for five individual experiments.

Table 1. The values of endotoxin level detected in different commercially available carbon-based nanomaterials (CBNs) was determined using ToxinSensorTM Chromogenic LAL Endotoxin Assay. (A) Endotoxin level in each material was measured at different concentration before and after centrifugation. Each material was also spiked with 0.1 EU of *E. coli* lipopolysaccharide (LPS) and retested for endotoxins before and after centrifugation. (B) Endotoxin spike recovery was calculated as the ratio of the actual level of endotoxins versus expected level before and after centrifugation and expressed as a percentage. Green cases show values outside the IEC range, and red cases show values within IEC ranges. Data shown as the mean values ± standard error of three independent experiments ($n = 3$). ¥, $P < 0.05$, versus non-spiked and non-centrifuged samples; †, $P < 0.05$, versus spiked and non-centrifuged samples

A

		Endotoxin level (Eu/ml±SE)			
		Non spiked		Spiked	
		Non Centrifuged	Centrifuged	Non Centrifuged	Centrifuged
	Water	0	0	0.39 ± 0.01	0.39 ± 0.02
Activated Carbon	10µg/ml	0.89 ± 0.09	0.10 ± 0.04 ¥	1.27 ± 0.17	0.31 ± 0.05 †
	1µg/ml	0.27 ± 0.09	0.11 ± 0.02 ¥	0.36 ± 0.02	0.24 ± 0.05
	0.1µg/ml	0.21 ± 0.05	0.08 ± 0.04 ¥	0.37 ± 0.05	0.21 ± 0.04 †
	0.01µg/ml	0.17 ± 0.05	0.06 ± 0.02	0.3 ± 0.06	0.19 ± 0.10
Graphene	10µg/ml	4.96 ± 0.17	1.13 ± 0.10 ¥	4.77 ± 0.10	2.41 ± 0.22 †
	1µg/ml	0.96 ± 0.003	0.75 ± 0.17	0.96 ± 0.01	0.54 ± 0.02 †
	0.1µg/ml	0.68 ± 0.01	0.46 ± 0.10 ¥	0.74 ± 0.02	0.54 ± 0.03 †
	0.01µg/ml	0.26 ± 0.02	0.20 ± 0.002 ¥	0.55 ± 0.02	0.54 ± 0.01
Helical MWCNT	10µg/ml	4.74 ± 0.34	0.31 ± 0.06 ¥	5.11 ± 0.53	1.04 ± 0.34 †
	1µg/ml	1.14 ± 0.09	0.08 ± 0.24 ¥	1.57 ± 0.21	0.33 ± 0.09 †
	0.1µg/ml	0.16 ± 0.01	0.16 ± 0.27	0.5 ± 0.04	0.22 ± 0.01 †
	0.01µg/ml	0.07 ± 0.02	0.01 ± 0.03 ¥	0.36 ± 0.12	0.23 ± 0.02
Long MWCNT	10µg/ml	6.64 ± 0.007	6.13 ± 0.005	6.16 ± 0.04	5.83 ± 0.06
	1µg/ml	4.74 ± 0.004	4.48 ± 0.012	5.87 ± 0.06	4.31 ± 0.19 †
	0.1µg/ml	1.97 ± 0.08	0.22 ± 0.02 ¥	2.08 ± 0.09	0.83 ± 0.03 †
	0.01µg/ml	0.13 ± 0.005	0.07 ± 0.02	0.90 ± 0.04	0.8 ± 0.09
Short MWCNT	10µg/ml	6.62 ± 0.04	5.7 ± 0.18	6.66 ± 0.33	5.38 ± 0.76
	1µg/ml	2.5 ± 0.04	0.53 ± 0.02 ¥	1.44 ± 0.57	1.05 ± 0.04
	0.1µg/ml	0.24 ± 0.01	0.14 ± 0.05 ¥	0.66 ± 0.09	0.26 ± 0.08 †
	0.01µg/ml	0.2 ± 0.08	0.24 ± 0.03	0.53 ± 0.16	0.17 ± 0.03 †
SWCNHs	10µg/ml	1.24 ± 0.05	0.83 ± 0.23	1.13 ± 0.01	1.13 ± 0.07
	1µg/ml	1.22 ± 0.07	0.64 ± 0.01 ¥	1.2 ± 0.02	1.03 ± 0.09
	0.1µg/ml	1.02 ± 0.05	0.5 ± 0.18 ¥	1.1 ± 0.06	1.24 ± 0.04
	0.01µg/ml	0.93 ± 0.02	0.30 ± 0.02 ¥	1.1 ± 0.06	1.02 ± 0.03

B

Endotoxin spike recovery %	
Spiked	
Non Centrifuged	Centrifuged
100%	100%
97%	54%
23%	33%
41%	33%
33%	33%
-49%	328%
-56%	38%
10%	33%
3%	10%
95%	187%
110%	64%
87%	15%
74%	56%
-123%	-77%
290%	-44%
28%	156%
197%	187%
10%	-82%
-272%	133%
108%	31%
85%	-18%
-28%	77%
-5%	100%
21%	190%
44%	185%

Statistical methods

Statistical analyses for cytotoxicity assays were conducted using GraphPad (GraphPad Software, Inc., La Jolla, CA, USA). The unpaired t-test was used to calculate statistical significance. For the pathway array experiments, statistical significance was calculated by using SA Biosciences online software. Differences were considered statistically significant at $P < 0.05$.

Results

Characterization of CBNs

Pristine graphene was characterized at NCTR and the University of Arkansas at Little Rock (Little Rock, AR, USA) and will be published as an independent manuscript. Specific characteristics such as purity and details of characterization of tubular CBNs were described in previous publications (Lahiani *et al.* 2016a, b). SWCNHs used in tests were synthesized and characterized in Center for Nanophase Materials Sciences, Oak Ridge National Laboratory as described by Lahiani *et al.* (2015). The Survey Scan for Elemental Analysis as well as analysis of C1s spectral regions for atomic environment/functional groups showed that the physical properties of the pristine graphene were not changed after the autoclaving (data not shown). A full manuscript describing the details of the characterization of pristine graphene is a part of the 'Special Issue on Graphene' and is published in the same journal.

Detection and quantification of endotoxin from pyrogenated and depyrogenated nanomaterials

Endotoxin levels were tested in the CBNs by employing both qualitative (LAL-gel clot) and quantitative (LAL chromogenic) assays. Raw NMs were suspended in depyrogenated water at a

Journal of AppliedToxicology

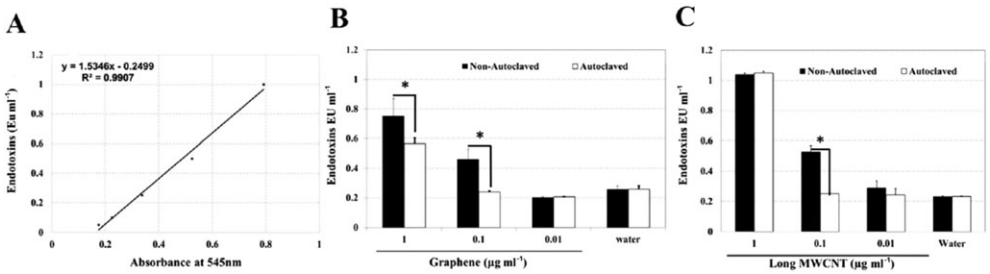

Figure 2. Depyrogenation of carbon-based nanomaterials (CBNs) decreases endotoxins levels. Standard curve was generated using lipopolysaccharide (LPS) standard (A). Autoclaving CBNs for three consecutive times can significantly decrease endotoxin contamination. Endotoxins level in graphene (B) and long multi-wall carbon nanotubes (MWCNTs) (C) before and after three times autoclaving. All data represent the mean of three independent experiments. Error bars represent standard error values.*, $P < 0.01$.

concentration of 100 μg ml^{-1}. Levels of endotoxin were measured in depyrogenated (autoclaved) and original (non-autoclaved) test materials. Activated carbon was used as a control for endotoxin testing.

As it is known that LPS can adhere to CBNs (Esch *et al*., 2010), the NMs solutions were further diluted for testing to 10, 1, 0.1 and 0.01 μg ml^{-1} in LAL reagent grade water. Results of the chromogenic LAL assay showed that even at the lowest concentration (0.01 μg ml^{-1}), traces of endotoxins were detected in the non-autoclaved CBNs. Moreover, the levels of endotoxins detected were not proportional to the dilutions used, which could imply an interference of CBNs with the LAL assay in use. To determine whether the endotoxins in a CBNs solution can be masked by the presence of the NMs, CBNs solutions were also tested after centrifugation. The gel-clot assay revealed that the 100, 10 and 1 μg ml^{-1} autoclaved uncentrifuged samples showed positive results (clot formation) for all the test samples (data not shown). After centrifugation, the amount of endotoxin in the supernatant of CBNs solutions decreased significantly as measured by the qualitative (gel clot assay; data not shown) as well as quantitative assay (Table 1A).

The FDA guidelines and the United States Pharmacopeia (USP) standard for the LAL test have mandated certain criteria (the spike recovery) for establishing the validity of the test (USP, 2007). To further confirm the interference of CBNs with the LAL assay, each CBNs sample was spiked with 0.1 EU of *E.coli* LPS, samples were evaluated via the chromogenic LAL assay, and recovery of the spiked endotoxin was calculated. The recovery of spiked endotoxin was measured in non-centrifuged, as well as centrifuged samples. According to FDA/USP guidelines, the IEC should exhibit a 50–200% spike recovery. When LAL-grade water was spiked with a known amount of LPS, the spike recovery was almost 100% (Table 1B). Further centrifugation of the water solution did not affect the recovery percentage. However, when the same amount of endotoxin was spiked into solutions containing the CBNs, the amount of detected endotoxin was either below 50% or above 200% of the spiked (theoretical) amount in 4 different CBNs materials: Graphene (all concentrations), long MWCNTs (10, 1 and 0.1 μg ml^{-1}), short MWCNTs (10 and 1 μg ml^{-1}) and SWCNHs (all concentrations). Helical MWCNTs, on the other hand, showed spike recovery values within the FDA/USP ranges. After centrifugation, the endotoxin recovered from spiked solutions was significantly lower than the non-centrifuged samples of graphene (10, 1 and 0.1 μg ml^{-1}), helical MWCNTs (10, 1 and 0.1 μg ml^{-1}), long MWCNT (1 and 0.1 μg ml^{-1}) and short MWCNT (0.1 and 0.01 μg ml^{-1}) (Table 1A). These results confirm the previous findings using non-spiked solutions and further suggest that there may be an interaction of LPS with the carbon NMs (binding of LPS with CBNs) and, therefore, CBNs interference with the LAL test.

A standard curve was generated using LPS standard (Fig. 2A). After triple autoclaving, 0.1 μg ml^{-1} graphene (Fig. 2B) and MWCNTs (Fig. 2C) had an acceptable level of endotoxin (0.2 EU ml^{-1}). This result indicates that autoclaving reduce/depyrogenate the amount of endotoxin. Moreover, autoclaved and centrifuged samples had acceptable levels of endotoxin (0.5 EU ml^{-1}) even at 1 μg ml^{-1} concentration of graphene (Fig. 2C). The non-centrifuged and autoclaved sample had an acceptable level of endotoxin at 0.1 μg/ml. The results from both methods suggest that autoclaving was able to reduce the level of endotoxin.

Table 2. Macrophages were exposed to different concentrations of carbon-based nanomaterials (pyrogenated and depyrogenated) and endotoxins

Experimental Group	Treatment	Concentration
Group 1	Endotoxin	1 EU
Group 2	Endotoxin	2 EU
Group 3	Graphene (Non-autoclaved)	1 μg ml^{-1}
Group 4	Graphene (Autoclaved)	1 μg ml^{-1}
Group 5	Graphene (Non-autoclaved)	20 μg ml^{-1}
Group 6	Graphene (Autoclaved)	20 μg ml^{-1}
Group 7	MWCNTs (Non-autoclaved)	1 μg ml^{-1}
Group 8	MWCNTs (Autoclaved)	1 μg ml^{-1}
Group 9	MWCNTs (Non-autoclaved)	20 μg ml^{-1}
Group 10	MWCNTs (Autoclaved)	20 μg ml^{-1}

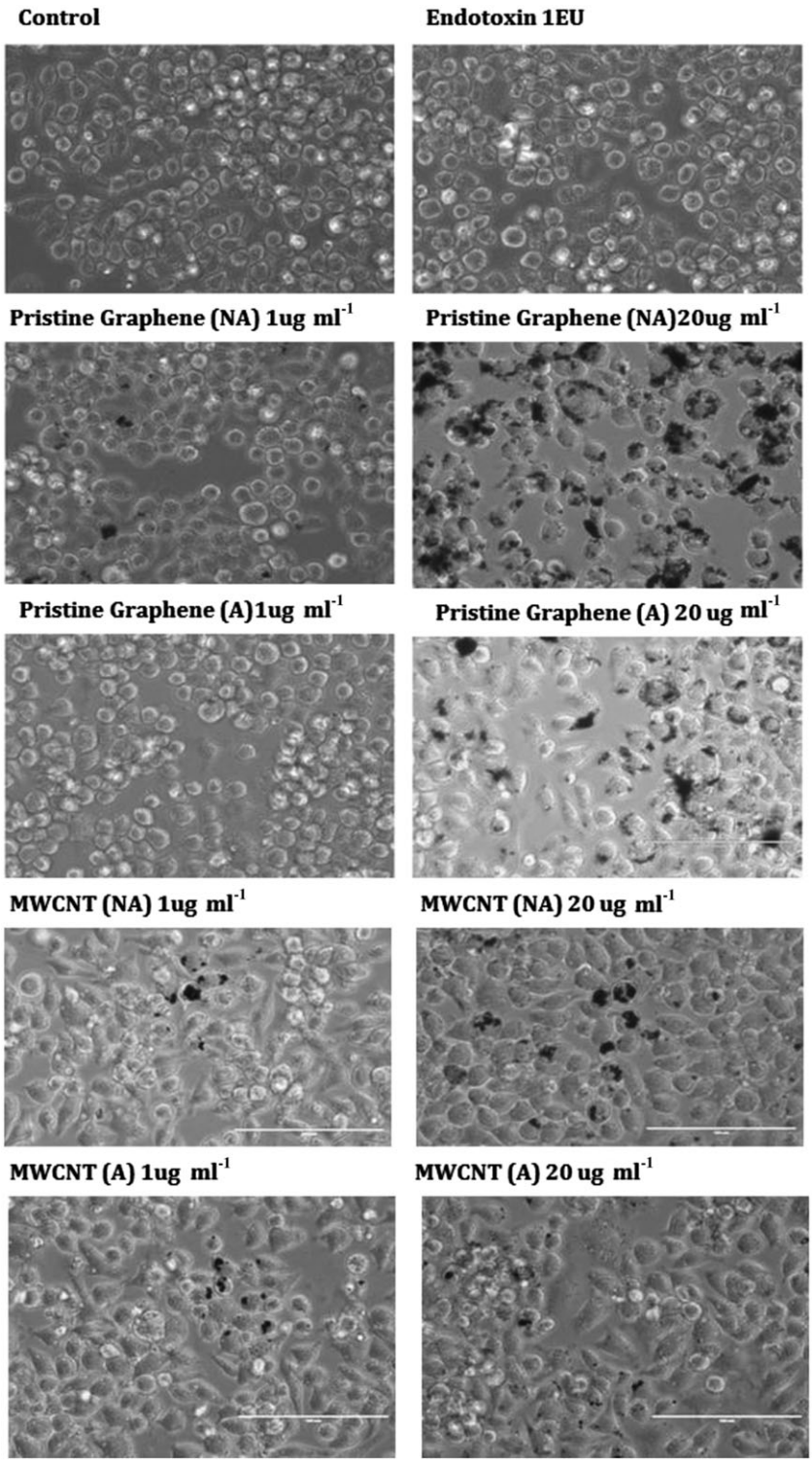

Figure 3. Uptake of depyrognated carbon-based nanomaterials (CBNs) by macrophages. Macrophages incubated with non-autoclaved CBNs showed a higher level of phagocytosis. J774 cells were incubated with non-autoclaved and with three times autoclaved CBNs. Cells visualized under 40× magnification.

The second method was spike recovery method, in which we spiked known amount of endotoxin in both autoclaved and non-autoclaved samples. The results show that spiked centrifuged autoclaved sample had an acceptable level of endotoxin in 0.1 μg ml^{-1} concentration of graphene. Whereas, the spiked non-centrifuged sample had an unacceptable level of endotoxin even at 0.01 μg ml^{-1} diluted sample in both autoclaved and non-autoclaved samples. This high level of endotoxin was due to spiking. Overall, these results indicate that the majority of the endotoxin is bound or trapped within CBNs. These results further indicate that autoclaving reduces the endotoxin level.

Journal of AppliedToxicology

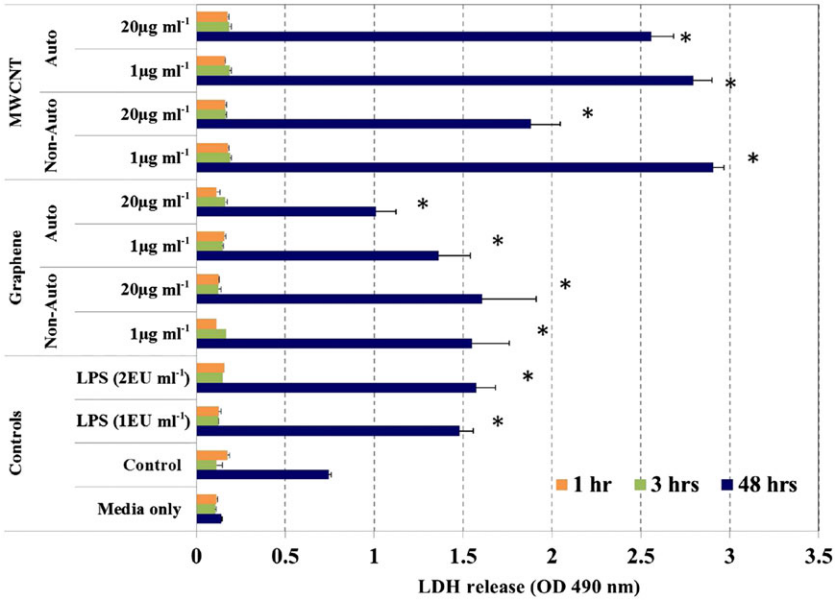

Figure 4. Pristine and depyrogenated carbon-based nanomaterials (CBNs) induce lactate dehydrogenase (LDH) to release in J774 cells. The effect of pyrogenated and depyrogenated CBNs on LDH release are shown. J774 cells (2×10^5 cells per well) were treated with either graphene (1 and 20 μg ml^{-1}) or long multi-wall carbon nanotubes (MWCNTs) (1 and 20 μg ml^{-1}) for 48 h *in vitro*. LDH release was determined as described in Materials and Methods at 1, 3 and 48 h post treatment. Data expressed as the mean of optical density values ± standard error of three independent experiments. *$P < 0.01$, versus untreated control (Control).

Phagocytosis

Next, we investigated if there was any difference in macrophage uptake of CBNs between autoclaved and non-autoclaved NMs. Test samples (Table 2) were incubated with two different concentrations (1 and 20 μg ml^{-1}). Images were captured 1, 3 and 48 h post incubation. The captured images clearly showed that macrophages engulfed more NMs when incubated with the non-autoclaved material than with the autoclaved material (Fig. 3). Furthermore, the CBNs appeared to be localized to vacuoles this was most obvious with the NA-MWCNTs as compared to NA-graphene (Supplementary Information Fig. 2). Autoclaved samples were engulfed in a lower amount as compared with non-autoclaved materials (Supplementary Information Fig. 2B, D). This result indicates that non-autoclaved NMs may be more antigenic due to the presence of contaminated endotoxin.

Cell cytotoxicity

The cytotoxic effects of graphene and MWCNTs on macrophages were determined by assessing LDH activity (Fig. 4). Untreated cells not incubated with any test compounds served as a negative control. Cytotoxicity was measured at four different time points (1, 3 and 48 h). No cytotoxicity was observed for the negative control cells, even after 48-h incubation. In this experiment two concentrations (1 and 2 EU ml^{-1}) of LPS was used as a positive control for cytotoxicity. Both concentrations of LPS caused cell cytotoxicity only after 48-h incubation. Next, we analysed the cytotoxicity of graphene for both pyrogenated and depyrogenated test material. The results indicated that both pyrogenated and depyrogenated CBNs was unable to cause cytotoxicity at the 1 and 3 h time points. In contrast, macrophages incubated for 24 and 48 h had significantly higher cytotoxicity as compared with 1- and 3-h incubation or control cells. The result also showed that the level of cytotoxicity was much higher at 48 h in comparison with 24 h during graphene incubation. Pyrogenated CBNs (both graphene and different MWCNTs) generally produced more LDH, indicating greater cell toxicity. This similar pattern was observed at both 1 and 20 μg ml^{-1} concentrations. The results showed that a similar pattern was observed in both graphene and MWCNTs, the primary difference that the 1 μg ml^{-1} concentration of pyrogenated or non-autoclaved MWCNTs induced macrophages to produce significantly higher LDH as compared with 20 μg ml^{-1} concentration.

Gene expression analysis

To assess the immunotoxicity of CBNs, macrophages were incubated with endotoxin (1 EU and 2 EU), pristine graphene (1 and 20 μg ml^{-1}; autoclaved and non-autoclaved), and MWCNTs (1 and 20 μg ml^{-1}; autoclaved and non-autoclaved). We then analyzed the differential expressions of immune response-related genes in macrophages. A heat map generated from the gene expression data (Fig. 5) showed that the pattern of gene expression mediated by CBNs segregated into autoclaved and non-autoclaved groups, as well as there was segregation for gene expression during graphene or MWCNTs mediated activation. Next, we performed a detailed analysis of altered gene expression between the experimental groups and endotoxin-treated group (positive control). Based on the observed gene expression pattern, we categorized results into three subgroups: (i) same genes differentially regulated in all groups, (ii) genes predominant in the macrophages treated with endotoxin and non-autoclaved test material, and (iii) genes common in the macrophages treated with CBNs (both graphene and MWCNTs). In the first subgroup (genes upregulated in all groups), the genes *TLR5, CXCL3, IL1b, IL6,* and *mefv* were found to be significantly downregulated. Only the expression of *IRF7* was upregulated. In the second subgroup, the positive control (endotoxin), as well as MWCNTs (NA), resulted in the activation of genes *ACPS, CRP, CXCL5, CTSG, DMBt1, IFNa9*

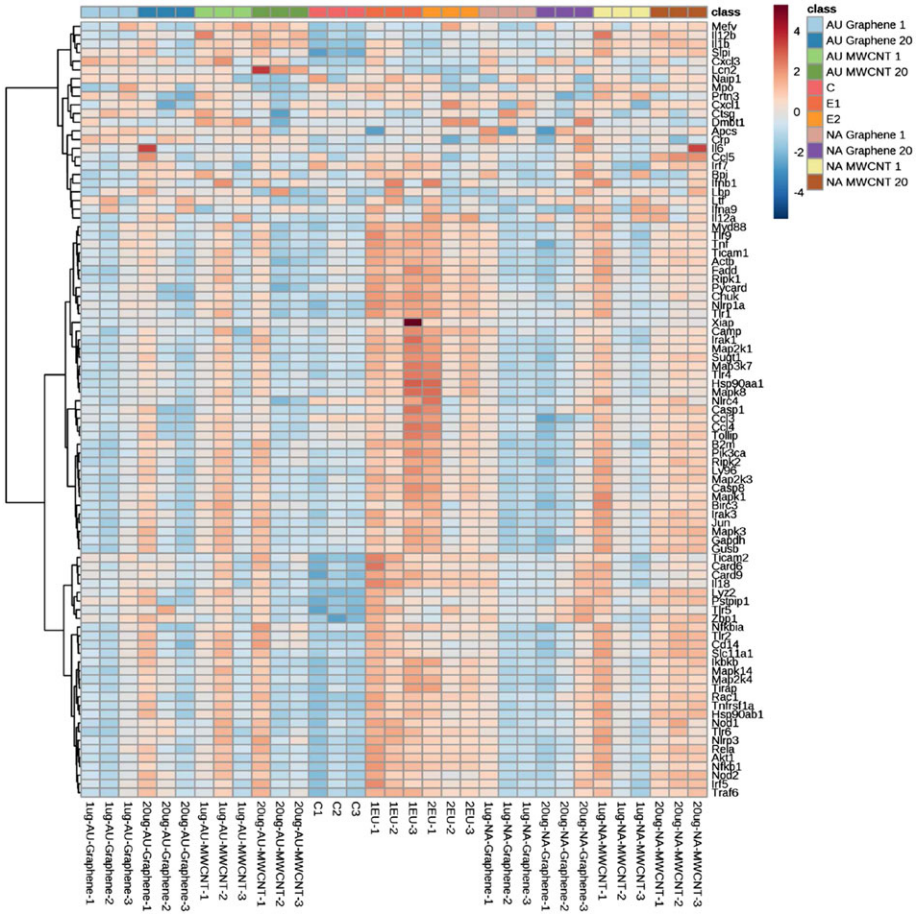

Figure 5. Heatmap depicting the expression of genes in various experimental groups. The effect of pyrogenated and depyrogenated carbon-based nanomaterials (CBNs) on the expression of genes involved in the immune response. J774 cells (2×10^5 cells per well) were treated with endotoxin (1EU and 2EU), autoclaved (AU) and non-autoclaved (NA) graphene (1 and 20 μg ml^{-1}) or multi-wall carbon nanotubes (MWCNTs) (1 and 20 μg ml^{-1}) for 48 h *in vitro*. The GUSB gene was used for the normalization of the data. Heat map was generated after autoscaling of the CT values (mean-centered and divided by the standard deviation of each variable).

and *MGDC*. The third subgroup (all CBNs) was marked by the differential expression of genes *CCL3, LYZ2, NLRC4* and *SLPI*. Interestingly, all of the test materials caused down-regulation of *CARD6* and *CARD9*, but only graphene (both autoclaved and non-autoclaved) demonstrated statistical significance.

Overall, the gene expression patterns clearly indicated that there was a distinct pattern of mRNA gene expression in macrophages treated with bacterial endotoxin (positive control), graphene, or MWCNTs. Moreover, there was a differential expression of pathogen recognition receptors, as well as downstream signaling molecules/effector molecules.

Discussion

Safety assessments of NMs could provide misleading and incorrect information if the NMs are contaminated with endotoxins or other bacterial contaminants. The current method of endotoxin detection using LAL reagent (Cooper *et al.*, 1970) was developed as an alternative to the pyrogenicity test using the *in vivo* rabbit model (Williams, 2007). These methods have been described in the pharmacopoeia of many countries (Smulders *et al.*, 2012). Nevertheless, many reports have demonstrated interference of engineered NM with one or more formats of the LAL test (Cooper, 1990; Bohrer *et al.*, 2001; Fujita *et al.*, 2011). Smulders and co-workers reported that some NMs, including TiO_2, Ag, $CaCO_3$, and SiO_2, interfere with the LAL test (Smulders *et al.*, 2012). Recently, Li *et al.* (2015) showed that the chromogenic LAL test was more accurate in the detection of endotoxins in solutions of Au, Ag, and iron oxide NMs than the turbidity-based and gel clot assays. Previously, it was shown that activated carbon, a carbon allotrope, can adsorb endotoxins (Du *et al.*, 1987). Recent studies have also tried to understand the interaction of endotoxins with CBNs (Esch *et al.*, 2010; Jackson *et al.*, 2015). However, the methodology of endotoxin detection used in the latter studies did not consider the fact that endotoxins can bind CBNs and, therefore, interfere with the LAL assay itself. The properties of the amphiphilic LPS molecule facilitates its interactions with other proteins, biomembranes, surface markers, and, likely, NMs (Carr and Morrison, 1984). However, the causes of inhibition or enhancement of endotoxin detection assays in NMs solutions are unknown (Dobrovolskaia *et al.*, 2010). Interestingly, in our study, the functionalized MWCNTs (long and short), which have carboxylic groups, had low recovery values. It has been demonstrated that carboxylic groups can electrostatically bind to the LPS and, therefore, lead to interference with endotoxin detection (Schromm *et al.*, 1998). Moreover, the helical MWCNTs used in the study, which was not functionalized, showed a recovery level within FDA/USP ranges of test validity.

Journal of AppliedToxicology

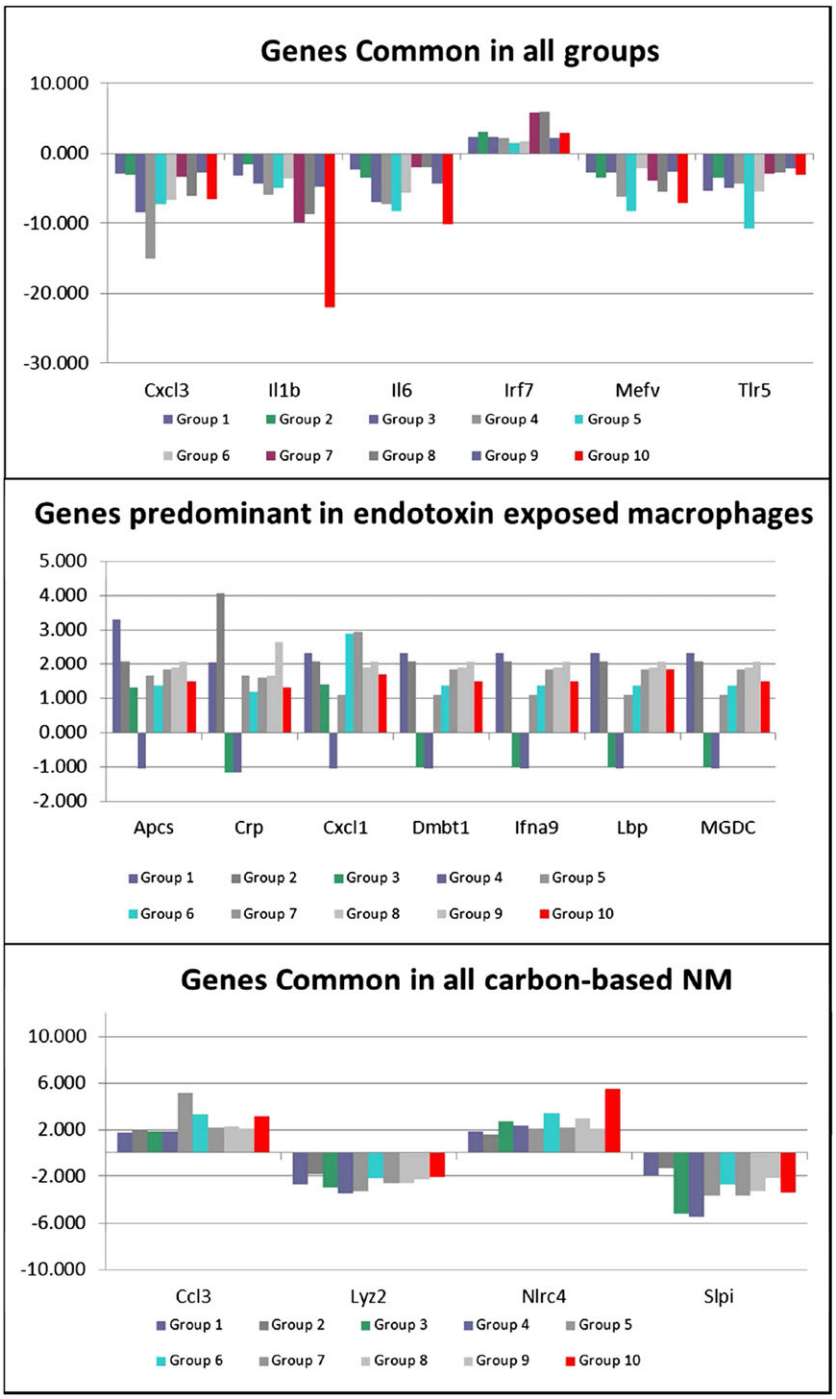

Figure 6. Pattern of gene expression during interaction of macrophages with endotoxin or carbon-based nanomaterials (CBNs). (A) same genes differentially regulated in all groups, (B) genes predominant in the macrophages treated with endotoxin or CBNs containing endotoxin, and (C) gene common in the macrophages treated with CBNs.

Some research groups have used a centrifugation approach to avoid interference of the NM with the LAL assay (Smulders *et al.*, 2012; Jackson *et al.*, 2015). However, such methodology does not take into account that the binding of LPS and other molecules to the NM surface could result in an underestimation of total endotoxin using this approach.

We next investigated if mouse macrophages have different phagocytic and cytotoxic response when exposed to pyrogenated or depyrogenated CBNs. The difference in phagocytosis is believed to be due to the presence of endotoxin in the graphene and MWCNTs. Earlier it has been shown that the administration of endotoxin increases the phagocytosis of alveolar macrophages (Frevert *et al.*, 1998). After the engulfment or phagocytosis of the CBNs, the next obvious question is whether these engulfed particles are cytotoxic to the cell. Our results showed that the MWCNTs were more toxic than the graphene. This could be due to the interaction of LPS with the functionalized MWCNTs. Higher amounts of LPS could have caused the increased phagocytosis

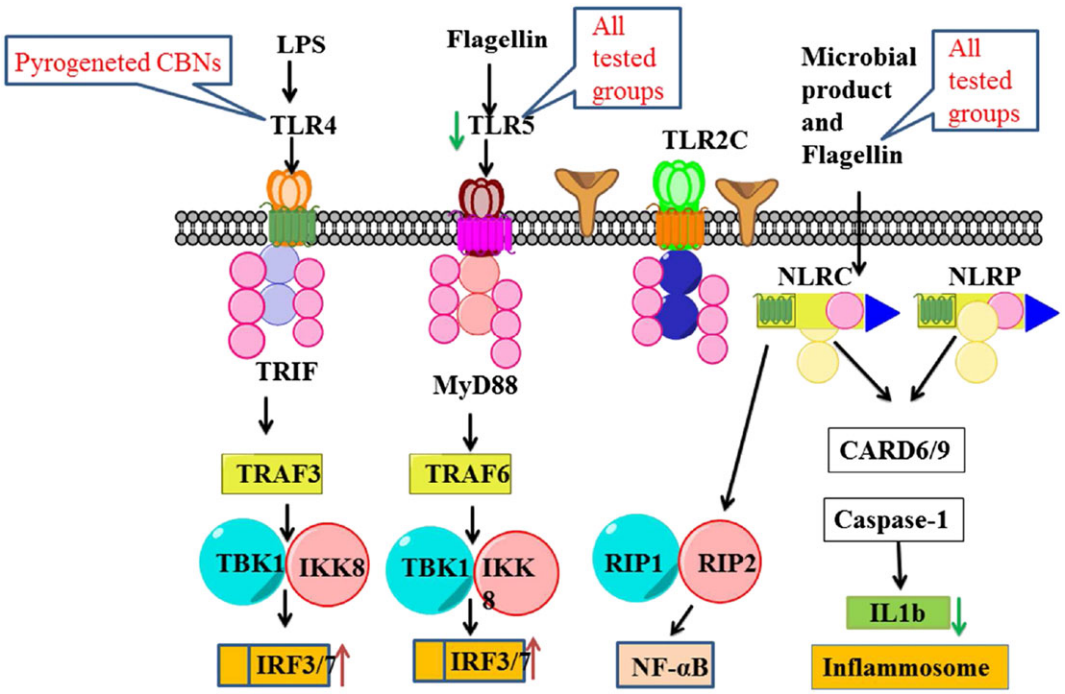

Figure 7. Schematic diagram showing the proposed mechanism of interaction of endotoxin and tested carbon-based nanomaterials (CBNs) with receptors on macrophages and activation of signaling molecules.

as well as higher LDH production—a hallmark of cytotoxicity. This cytotoxicity could be a result of the binding of LPS to surface receptors on the macrophages. Endotoxin is a large molecule derived from outer membrane components of Gram-negative bacteria, containing a polysaccharide part and a lipid part. This pyrogenic molecule activates various genes involved in the innate immune response. Immune cells sense the triggering molecules (in our study, believed to be associated with the CBNs) via the pattern recognition receptors (PRR) that are present on the cell surface of immune cells. Toll-like receptors (TLR) and Nod-like receptors (NLR) recognize the triggering molecules through pathogen-associated molecular patterns (PAMP). TLR also serves as a bridge between innate and adaptive immunity. Studies have shown different levels of crosstalk between TLRs and NLR signaling pathways of immune cells. The LPS can bind to toll-like receptor 4 (TLR4) and activate macrophages and monocytes. The binding to TLR4 receptors induces an intracellular signaling pathway mediated by the *Myeloid Differentiation Primary Response 88* (MyD88), *Janus Kinase (JAK) quinases,* and *Signal Transducer and Activation of Transcription* (*STATS*) proteins that lead to activation of transcription factors *Nuclear factor Kappa β (NFKβ)* and proinflammatory cytokines such as *IL-1β* and *TNF-α* (Chow *et al.*, 1999; Zhou *et al.*, 2004; Murshid *et al.*, 2015) and cellular functions.

Interestingly, all of the tested material prompted a down-regulation of the TLR4 receptor. However, statistical significance was achieved only in the endotoxin-treated macrophages. Furthermore, the gene expression of LPS binding protein (LBP) was downregulated in macrophages exposed to both endotoxin and NA-MWCNTs. This clearly indicates that the LPS in the MWCNTs may be responsible for this binding. LPS can bind to the C-reactive protein and may cause activation of several cytokines (Tan *et al.*, 2005) as shown in Fig. 6B.

The most interesting finding of this study was the downregulation of the TLR5 gene after exposure of macrophages with any of the test agent. TLR5 binds to the bacterial protein flagellin; therefore it is very important to distinguish between bacterial LPS and bacterial flagellin contamination. For the safety of NMs and biological preparations containing such materials, the emphasis has been given to remove the endotoxin by several procedures (Magalhaes *et al.*, 2007). The findings of our study clearly indicate that decontamination methods need to be established beyond the removal of endotoxin from such materials.

The interaction of *TLR4* or *TLR5* with contaminant present in the CBNs may lead to the modulation of *TRAF3* or *TRAF6,* respectively, which leads to further activation of *IRF3/7* or *NF-kB* and production of *IFNβ/α* or other proinflammatory cytokines (Fig. 7). The upregulation of IRF7, which is a crucial regulator of type I interferons, provides evidence for its role in the regulation and activation of immune responses exerted by the test substances. Both graphene and MWCNTs caused higher expression of the *NLRC4* inflammasome. The *NLRC4* inflammasome is known to detect the cytosolic/intracellular presence of bacterial products and components, specifically bacterial flagellin (Zhao *et al.*, 2011). This interaction further leads to the activation of several inflammatory cytokines. The higher expression of the *NLRC4* inflammasome in this study further confirms the importance of proper assessment of bacterial contaminants in biological products containing CBNs. In conclusion, this study found that CBNs including pristine graphene and MWCNTs tested positive for endotoxins by different methods. Measurement of the supernatant after centrifugation decreased the endotoxins level significantly, suggesting that endotoxins may be binding to these nanoparticles. For many of the NMs tests, calculated; levels of endotoxins were higher than the 0.5 EU ml^{-1} level approved by the FDA for medical products.

All CBNs caused increased LDH production in macrophages, a marker for cytotoxicity. Of the test materials, MWCNTs prompted the greatest cytotoxicity. Both graphene and MWCNTs showed

maximum cytotoxicity after 48-h incubation. Depyrogenation reduced the toxicity of all tested CBNs. Macrophages incubated with Pristine CBNs showed higher levels of phagocytosis and material appeared to be localized to vacuoles. This pattern was even more apparent with MWCNTs. There was also a distinct profile of mRNA gene expression in macrophages treated with bacterial endotoxin (positive control), graphene, or MWCNTs compared with the negative controls. Moreover, they had differential expression of PRR and downstream signaling molecules/effector molecules. TLR5 recognizes the extracellular flagellin and induces differential expression of proinflammatory cytokines, whereas *Nod-like receptor* (*NLR*) and the *NLRP4* inflammasome recognize the flagellin present within the macrophages and activate Caspases and expression of IL1β (Fig. 7). Researchers should take care to ensure that depyrogenated NMs are used for studies involving immunologic approaches. Scientists should also be cautious in interpreting results and reports on the aggravating effects of CBNs for adverse health without corresponding data describing materials testing for endotoxin and manufacturing conditions.

Acknowledgments

Authors would like to thank Drs. Carl Cerniglia, Jyotsanbala Kanungo and Kidon Sung (NCTR/US-FDA) for the critical review of this manuscript. Experiments with graphene is part of Arkansas Research Consortium in Nanotoxicity (ARCN) and were supported by funds from NCTR/US-FDA (grant for Sangeeta Khare). Mohamed Lahiani was a UALR graduate student and participant of guest worker appointment at NCTR. The stipend for Mohamed Lahiani and a part of work performed on SWCNHs; short, long, helical MWCNTs was funded by Arkansas Science & Technology Authority (ASTA) (grant for Mariya Khodakovskaya). Kuppan Gokulan and Katherine Williams were supported by Oak Ridge Institute for Science and Education (ORISE) research appointment. We acknowledge the help provided by the NanoCore facility at NCTR to procure pristine graphene and characterize it, and Shawn Bourdo (Center for Integrative Nanotechnology Sciences at UALR) for characterizing pristine and autoclaved graphene. We are also grateful to Center for Nanophase Materials Sciences CNMS for providing SWCNHs used in the current study (collaborative agreement between UALR and CNMS).

Conflict of Interest

The authors did not report any conflict of interest.

Disclaimer

The findings and conclusions expressed in this manuscript are those of the authors and do not necessarily represent the views of the US Food and Drug Administration.

References

Adibkia K, Omidi Y, Siahi MR, Javadzadeh AR, Barzegar-Jalali M, Barar J, Maleki N, Mohammadi G, Nokhodchi A. 2007. Inhibition of endotoxin-induced uveitis by methylprednisolone acetate nanosuspension in rabbits. *J. Ocul. Pharmacol. Ther.* **23**: 421432.

Alex S, Tiwari A. 2015. Functionalized Gold Nanoparticles: Synthesis, Properties and Applications--A Review. *J. Nanosci. Nanotechnol.* **15**: 1869–1894.

Amenta V, Aschberger K. 2015. Carbon nanotubes: potential medical applications and safety concerns. *Wiley Interdiscip. Rev. Nanomed. Nanobiotechnol.* **7**: 371–386.

Aslani F, Bagheri S, Muhd Julkapli N, Juraimi AS, Hashemi FS, Baghdadi A. 2014. Effects of engineered nanomaterials on plants growth: an overview. *ScientificWorldJournal* **2014**: 641759.

Bae KH, Chung HJ, Park TG. 2011. Nanomaterials for cancer therapy and imaging. *Mol Cells* **31**: 295–302.

Barbosa GM, Fagan SB, Martinez DST, Alves OL, Rodrigues Junior LC. 2015. Lipopolysaccharide influences on the toxicity of oxidised multiwalled carbon nanotubes to murine splenocytes in vitro. *J. Exp. Nanosci.* **10**: 729–737.

Bekele AZ, Gokulan K, Williams KM, Khare S. 2016. Dose and Size-Dependent Antiviral Effects of Silver Nanoparticles on Feline Calicivirus, a Human Norovirus Surrogate. *Foodborne Pathog. Dis.* **13**: 239–244.

Bianco A, Kostarelos K, Prato M. 2005. Applications of carbon nanotubes in drug delivery. *Curr. Opin. Chem. Biol.* **9**: 674–679.

Bohrer D, Horner R, do Nascimento PC, Adaime M, Pereira ME, Martins AF, Hartz SA. 2001. Interference in the Limulus amebocyte lysate assay for endotoxin determination in peritoneal dialysis fluids and concentrates for hemodialysis. *J. Pharm. Biomed. Anal.* **26**: 811–818.

Canas JE, Long M, Nations S, Vadan R, Dai L, Luo M, Ambikapathi R, Lee EH, Olszyk D. 2008. Effects of functionalized and nonfunctionalized single-walled carbon nanotubes on root elongation of select crop species. *Environ. Toxicol. Chem.* **27**: 1922–1931.

Carr C, Jr, Morrison DC. 1984. Lipopolysaccharide interaction with rabbit erythrocyte membranes. *Infect. Immun.* **43**: 600–606.

Cha C, Shin SR, Annabi N, Dokmeci MR, Khademhosseini A. 2013. Carbon-based nanomaterials: multifunctional materials for biomedical engineering. *ACS Nano* **7**: 2891–2897.

Che Abdullah CA, Azad CL, Ovalle-Robles R, Fang S, Lima MD, Lepro X, Collins S, Baughman RH, Dalton AB, Plant NJ, Sear RP. 2014. Primary liver cells cultured on carbon nanotube substrates for liver tissue engineering and drug discovery applications. *ACS Appl. Mater. Interfaces* **6**: 10373–10380.

Chow JC, Young DW, Golenbock DT, Christ WJ, Gusovsky F. 1999. Toll-like receptor-4 mediates lipopolysaccharide-induced signal transduction. *J. Biol. Chem.* **274**: 10689–10692.

Cooper JF. 1990. Resolving LAL Test interferences. *J. Parenter. Sci. Technol.* **44**: 13–15.

Cooper JF, Levin J, Wagner HN. 1970. New rapid in vitro test for pyrogen in short-live radiopharmaceuticals. *J. Nucl. Med.* **11**: 310.

Dizaj SM, Mennati A, Jafari S, Khezri K, Adibkia K. 2015. Antimicrobial Activity of Carbon Based Nanoparticles. *Adv. Pharm. Bull.* **5**: 19–23.

Dobrovolskaia MA, Neun BW, Clogston JD, Ding H, Ljubimova J, McNeil SE. 2010. Ambiguities in applying traditional Limulus amebocyte lysate tests to quantify endotoxin in nanoparticle formulations. *Nanomedicine (Lond)* **5**: 555–562.

Du XN, Niu Z, Zhou GZ, Li ZM. 1987. Effect of activated charcoal on endotoxin adsorption. Part I. An in vitro study. *Biomater. Artif. Cells Artif. Organs* **15**: 229–235.

Esch RK, Han L, Foarde KK, Ensor DS. 2010. Endotoxin contamination of engineered nanomaterials. *Nanotoxicology* **4**: 73–83.

Frevert CW, Warner AE, Weller E, Brain JD. 1998. The effect of endotoxin on in vivo rat alveolar macrophage phagocytosis. *Exp. Lung Res.* **24**: 745–758.

Fujita Y, Tokunaga T, Kataoka H. 2011. Saline and buffers minimize the action of interfering factors in the bacterial endotoxins test. *Anal. Biochem.* **409**: 46–53.

Gokulan K, Khare S, Williams K, Foley SL. 2016. Transmissible Plasmid Containing Salmonella enterica Heidelberg Isolates Modulate Cytokine Production During Early Stage of Interaction with Intestinal Epithelial Cells. *DNA Cell Biol.* **35**: 443–453.

Green AA, Hersam MC. 2011. Properties and application of double-walled carbon nanotubes sorted by outer-wall electronic type. *ACS Nano* **5**: 1459–1467.

Harrison BS, Atala A. 2007. Carbon nanotube applications for tissue engineering. *Biomaterials* **28**: 344–353.

Jackson P, Kling K, Jensen KA, Clausen PA, Madsen AM, Wallin H, Vogel U. 2015. Characterization of genotoxic response to 15 multiwalled carbon nanotubes with variable physicochemical properties including surface functionalizations in the FE1-Muta(TM) mouse lung epithelial cell line. *Environ. Mol. Mutagen.* **56**: 183–203.

Lahiani MH, Eassa S, Parnell C, Nima Z, Ghosh A, Biris AS, Khodakovskaya MV. 2016a. Carbon nanotubes as carriers of *Panax ginseng* metabolites and enhancers of ginsenosides Rb1 and Rg1 anti-cancer activity. *Nanotechnology* **28**: 015101.

Lahiani MH, Chen J, Irin F, Puretzky AA, Green MJ, Khodakovskaya MV. 2015. Interaction of carbon nanohorns with plants: Uptake and biological effects. *Carbon* **81**: 607–619.

Lahiani MH, Dervishi E, Ivanov I, Chen J, Khodakovskaya M. 2016b. Comparative study of plant responses to carbon-based nanomaterials with different morphologies. *Nanotechnology* **27**: 265102.

Li Y, Italiani P, Casals E, Tran N, Puntes VF, Boraschi D. 2015. Optimising the use of commercial LAL assays for the analysis of endotoxin contamination in metal colloids and metal oxide nanoparticles. *Nanotoxicology* **9**: 462–473.

Madani SY, Naderi N, Dissanayake O, Tan A, Seifalian AM. 2011. A new era of cancer treatment: carbon nanotubes as drug delivery tools. *Int. J. Nanomedicine* **6**: 2963–2979.

Magalhaes PO, Lopes AM, Mazzola PG, Rangel-Yagui C, Penna TC, Pessoa A, Jr. 2007. Methods of endotoxin removal from biological preparations: a review. *J. Pharm. Pharm. Sci.* **10**: 388–404.

Murshid A, Gong J, Calderwood S. 2015. LPS-activated Scavenger Receptor SREC-I can Induce entry of TLR4 into Lipid Microdomains, Mediate Signal Transduction and trigger cytokine release. *FASEB J.* **29**: 888.25.

Puretzky AA, Eres G, Rouleau CM, Ivanov IN, Geohegan DB. 2008. Real-time imaging of vertically aligned carbon nanotube array growth kinetics. *Nanotechnology* **19**: 055605.

Qu G, Liu S, Zhang S, Wang L, Wang X, Sun B, Yin N, Gao X, Xia T, Chen J-J. 2013. Graphene oxide induces toll-like receptor 4 (TLR4)-dependent necrosis in macrophages. *ACS Nano* **7**: 5732–5745.

Schaumberger S, Ladinig A, Reisinger N, Ritzmann M, Schatzmayr G. 2014. Evaluation of the endotoxin binding efficiency of clay minerals using the Limulus Amebocyte lysate test: an in vitro study. *AMB Express* **4** 1-0855-4-1.

Schromm AB, Brandenburg K, Loppnow H, Zahringer U, Rietschel ET, Carroll SF, Koch MH, Kusumoto S, Seydel U. 1998. The charge of endotoxin molecules influences their conformation and IL-6-inducing capacity. *J. Immunol.* **161**: 5464–5471.

Smulders S, Kaiser JP, Zuin S, Van Landuyt KL, Golanski L, Vanoirbeek J, Wick P, Hoet PH. 2012. Contamination of nanoparticles by endotoxin: evaluation of different test methods. *Part. Fibre Toxicol.* **9**: 41.

Tan SS, Ng PM, Ho B, Ding JL. 2005. The antimicrobial properties of C-reactive protein (CRP). *J. Endotoxin Res.* **11**: 249–256.

Tiwari PM, Vig K, Dennis VA, Singh SR. 2011. Functionalized Gold Nanoparticles and Their Biomedical Applications. *Nano* **1**: 31–63.

Tsai CY, Lu SL, Hu CW, Yeh CS, Lee GB, Lei HY. 2012. Size-dependent attenuation of TLR9 signaling by gold nanoparticles in macrophages. *J. Immunol.* **188**: 68–76.

US-FDA. 2012. Guidance for Industry: Pyrogen and Endotoxins Testing. http://www.fda.gov/Drugs/GuidanceComplianceRegulatoryInformation/Guidances/ucm314718.htm (accessed on 08/01/2015).

Usp <85> Bacterial endotoxins test. 2007. http://www.usp.org/usp-nf/harmonization/stage-6/bacterial-endotoxins-test.

Vallhov H, Qin J, Johansson SM, Ahlborg N, Muhammed MA, Scheynius A, Gabrielsson S. 2006. The importance of an endotoxin-free environment during the production of nanoparticles used in medical applications. *Nano Lett.* **6**: 1682–1686.

Vance ME, Kuiken T, Vejerano EP, McGinnis SP, Hochella MF, Jr, Rejeski D, Hull MS. 2015. Nanotechnology in the real world: Redeveloping the nanomaterial consumer products inventory. *Beilstein J. Nanotechnol.* **6**: 1769–1780.

Vives-Pi M, Somoza N, Fernandez-Alvarez J, Vargas F, Caro P, Alba A, Gomis R, Labeta MO, Pujol-Borrell R. 2003. Evidence of expression of endotoxin receptors CD14, toll-like receptors TLR4 and TLR2 and associated molecule MD-2 and of sensitivity to endotoxin (LPS) in islet beta cells. *Clin. Exp. Immunol.* **133**: 208–218.

Wang K, Ruan J, Song H, Zhang J, Wo Y, Guo S, Cui D. 2011. Biocompatibility of Graphene Oxide. *Nanoscale Res. Lett.* **6**: 8.

Williams KM, Gokulan K, Cerniglia CE, Khare S. 2016. Size and dose dependent effects of silver nanoparticle exposure on intestinal permeability in an in vitro model of the human gut epithelium. *J. Nanobiotechnology* **14**: 62.

Williams KM, Milner J, Boudreau MD, Gokulan K, Cerniglia CE, Khare S. 2015. Effects of subchronic exposure of silver nanoparticles on intestinal microbiota and gut-associated immune responses in the ileum of Sprague-Dawley rats. *Nanotoxicology* **9**: 279–289.

Williams KL. 2007. Limulus amebocyte lysate discovery, mechanism and application. In *Endotoxins: Pyrogens LAL Testing, and Depyrogenation*, Williams KL (ed). CRC Press; 191–220.

Ying X. 2006. Inhibition of *E. coli* and Adsorption of Endotoxin by Modified Silicates and Carbo Nanotubes with Cetylpyridinium Chloride. Master thesis. Huazhong Agricultural University, ID: 1078909.

Zhang M, Yamaguchi T, Iijima S, Yudasaka M. 2013. Size-dependent biodistribution of carbon nanohorns in vivo. *Nanomed. Nanotech. Biol. Med.* **9**: 657–664.

Zhao Y, Yang J, Shi J, Gong YN, Lu Q, Xu H, Liu L, Shao F. 2011. The NLRC4 inflammasome receptors for bacterial flagellin and type III secretion apparatus. *Nature* **477**: 596–600.

Zhou H, Ding G, Liu W, Wang L, Lu Y, Cao H, Zheng J. 2004. Lipopolysaccharide could be internalized into human peripheral blood mononuclear cells and elicit TNF-alpha release, but not via the pathway of toll-like receptor 4 on the cell surface. *Cell. Mol. Immunol.* **1**: 373–377.

Zhou X, Torabi M, Lu J, Shen R, Zhang K. 2014. Nanostructured energetic composites: synthesis, ignition/combustion modeling, and applications. *ACS Appl. Mater. Interfaces* **6**: 3058–3074.

Supporting information

Additional Supporting Information may be found online in the supporting information tab for this article.